IEEE Access
Multidisciplinary | Rapid Review | Open Access Journal

SPECIAL SECTION ON MISSION CRITICAL PUBLIC-SAFETY COMMUNICATIONS: ARCHITECTURES, ENABLING TECHNOLOGIES, AND FUTURE APPLICATIONS

Received August 8, 2017, accepted August 30, 2017, date of publication September 6, 2017, date of current version September 27, 2017.

Digital Object Identifier 10.1109/ACCESS.2017.2749482

M^3-Cast: A Novel Multicast Scheme in Multi-Channel and Multi-Rate WiFi Direct Networks for Public Safety

GUL ZAMEEN KHAN[1], (Member, IEEE), EUN-CHAN PARK[2], (Member, IEEE), AND RUBEN GONZALEZ[1], (Member, IEEE)

[1]School of ICT, Griffith University, Gold Coast, QLD 4215, Australia
[2]Department of Information and Communication Engineering, Dongguk University, Seoul 04620, South Korea

Corresponding author: Eun-Chan Park (ecpark@dongguk.edu)

This work was supported by the Basic Science Research Program through the National Research Foundation of Korea funded by the Ministry of Science and ICT under Grant 2017R1A2B4009458.

ABSTRACT WiFi direct (WD) network is of significant interest during public safety scenarios due to its easy, quick, and efficient implementation. WD provides device to device communication using the MAC and PHY layers specifications of 802.11 standards, which facilitate multiple communications channels and a number of transmission rates to cope with the requirements and challenges of emerging applications in public safety and disaster management. Although they achieve substantial benefits in terms of high throughput, it creates a performance anomaly problem, wherein the selection of a particular communication channel and transmission rate can significantly affect the performance of a wireless communication system. This paper investigates the problem of selecting the most favorable channel and rate for a multicast communication system in the context of public safety using a WD 802.11 network. To this end, M^3-Cast protocol is proposed, which refers to a novel multi-rate multi-channel multicast scheme. M^3-Cast not only chooses the most favorable communication channel and transmission rate, but also considers the implementation details of the underlying WD technology, thereby optimizing the overall system performance. M^3-Cast is formulated analytically and evaluated by a complete system level simulation. The detailed results and the analysis considers a number of performance metrics, such as bit error rate, multicast capacity, and system throughput under different multiple input multiple output configurations, channel bandwidths, and various network radii. Consequently, the simulation and analytical results show that M^3-Cast protocol outperforms the standard multicast protocol of WD by almost twofold in terms of system throughput.

INDEX TERMS Public safety, WiFi direct, communication channels, transmission rate, multicast communication,D2D, wireless LAN, peer-to-peer.

I. INTRODUCTION

In recent years, Device to Device (D2D) communication has emerged as one of the most promising technologies in almost all popular wireless networks (i.e., Cellular Networks, WiFi, Bluetooth, and Zigbee etc). The D2D network attains several advantages such as increased spectral efficiency, high throughput, and reduced communication delay [1]. WiFi Direct (WD), developed by WiFi alliance, is a new state of the art technology for a D2D communication in a 802.11 network [2]. It is also known as a Peer-to-Peer (P2P) communication network. The WD provides connectivity between two or more WiFi enabled devices in the absence of an Access Point (AP). It is currently used in many applications such as local file sharing, printing, syncing, displaying content from one device to another, and many more applications [2]. Similarly, D2D can also serve as a technology component for providing Public Protection and Disaster Relief (PPDR) and National Security and Public Safety (NSPS) services [3]. In addition, WD provides instant, quick, easy and cheap connection in relation to mission-critical communications for public safety and can be inter networked with LTE networks for high performance and seamless user experience [4].

Multicast communication allows transfer of data from one device to two or more devices simultaneously. It is more efficient, faster, and cheaper compared to unicast

communication. Multicast in WD has emerged as an attractive feature of this new technology due to its useful applications such as local contents sharing, sharing network services, playing multi-player games, and a number of other proximity based services in public safety [5]. Similarly in the context of Internet of Things (IoT), WD multicast has numerous potential applications in various fields, viz. health, sports, agriculture, transportation, and gaming etc [6]. Multicast in WD can also be used in Vehicle to Vehicle (V2V) and Vehicle-to-anything (V2X) communications [7]. The new amendment of IEEE standard 802.11 for a Wireless Local Area Network (WLAN) i.e., 802.11ac achieves Very High Throughput (VHT) with the help of enhanced frame aggregation techniques at MAC layer, wider channel bandwidth, higher order modulation and coding schemes, higher number of Multiple Input Multiple Output (MIMO) and Multi User (MU)-MIMO at Physical (PHY) layer [8]. Furthermore, we loosely coin a term 802.11ac WD in this paper for the purpose of simplicity and clarity. The 802.11ac WD refers to a WD technology used with the specifications of the MAC and PHY layers of 802.11ac.

Yet in spite of its useful applications, multicast in WD faces many problems and issues including but not limited to reliability and efficiency. Although there is not much research on multicast in WD, the problem of multicast in standard WiFi[1] has been extensively explored in the literature. The WD specifications [2] does not add any new protocol for a multicast communication, instead it extends the regular multicast protocol of standard 802.11 to WD. Thus the related work for this paper investigates the multicast protocols of standard WiFi and the use of WD for public safety. This paper addresses the problem of choosing the most favourable transmission channel and rate for multicast communication in WD networks for public safety. For this purpose, M^3-Cast protocol is proposed, which is a novel **M**ulti-rate **M**ulti-channel **M**ulticast scheme in such a manner as to increase the overall system performance of WD networks for public safety.

The remainder of this paper is organized as follows: Section II describes the related work and the major contributions. The background overview and motivation are discussed in Section III. Next, Section IV describes the proposed M^3-Cast protocol. The analytical model is formulated in Section V. Then results and discussions are presented in Section VI. Lastly, the paper is concluded in Section VII.

II. RELATED WORK AND CONTRIBUTIONS

A considerable amount of literature has been published on the problems of multicast in 802.11 [9]. The two major problems in multicast in WiFi are reliability and efficiency. When we talk about reliability, our main objective is to reduce the losses due to collision and weak signals at the MAC and PHY layers, respectively. On the other hand, efficiency deals with the issues which arise from the multi-rate capability of different devices. In [10], the authors proposed a heuristic channel allocation algorithm to avoid the problem of hidden channel that arises from channel bonding of multiple 20 MHz channels in 5 GHz band in 802.11ac. Although the algorithm reduces Packet Error Rate (PER), the channel allocation scheme only takes into account the channel bonding scenario and does not provide any benefits if a channel has to be chosen from a pool of channels in case of multicast communication without channel bonding.

Similarly, the problem of improving public safety, using D2D communication, has attracted a lot attention recently. Many authors have addressed the issues of D2D communication in 5G and LTE in the context of public safety. In [11], an overview of Isolated E-UTRAN Operation for Public Safety (IOPS), its use cases, the network establishment and configuration specifications, user equipment (UE) configuration, security considerations, and mobility scenarios are discussed in detail. Similarly, the issues of user association in multi-tier heterogeneous networks (HetNets) and D2D discovery schemes for proximity-based services in LTE are investigated for public safety in [12] and [13]. In addition, with the emergence of WD technology, many researchers exploit the enhanced interworking between LTE and WD for adequate emergency group communication in public safety scenarios [4]. Likewise, [14] provides a solution for the creation of multiple, connected groups of Android devices to create close communication groups for public safety. However, the use of WD for public safety has not yet been explored from a complete system perspective in the context of the MAC and PHY layers.

A number of papers have investigated the multi-rate multicast in WLAN using different approaches. A major portion of the preliminary work on exploring multi-rate capability in multicast is based on combining Leader Based Protocols (LBP) and Automatic Rate Fallback (ARF) algorithms. In LBP [15], a leader is selected among the receivers in the multicast group. The leader then sends feedback information to the sender on behalf of the other receivers. Thus the sender and the group leader exchange Ready To Send (RTS) and Clear to Send (CTS) messages before the multicast communication. Similarly, the leader sends acknowledgement (ACK) messages after a successful reception of multicast data. On the contrary, the other receivers may send Negative Clear to Send (NCTS) and Negative acknowledgement (NACK) in case of failure of CTS and ACK messages, respectively. The authors in [16], used a leader-based mechanism (LB-ARF) in which the sender adjusts its transmission rate according to the feedback of the leader. Although, the author used Internet Group Management Protocol (IGMP) to elect the leader to make sure that a receiver with the lowest Signal to Interference and Noise Ratio (SINR) is chosen as a leader. However, it does not take into account the multi-channel environment. Similarly, [17] proposed SNR-based Auto Rate for Multicast (SARM), which chooses a node with the worst channel conditions as the leader of the multicast group. SARM is also

[1]A standard WiFi refers to 802.11 protocol that doesn't support a WD protocol.

more efficient in combating the collision due to its selection of backoff timer for each station, which is based on the received SNR. However, the main problem of the SARM is its dependency on beacon frames. In addition, the rate of a multicast transmission can not be changed if the channel conditions vary during the transmission of two consecutive beacon frames.

Likewise, Choi *et al.* [18] introduced the Probing-based Automatic Rate Fallback (PARF) mechanism in which a multicast sender adapts its transmission rate based on the channel conditions of all receivers in the multicast group. However, it does not improve performance substantially than those of the LBP and ARF protocols. Similarly, [19] provides a cross-layer auto rate selection multicast (ARSM) mechanism that adapts the rate according to varying channel conditions of the leader. In the same way, many other proposal have been reported in the literature for multi-rate adaptation in a multicast communication. However, these protocols consider a single channel while choosing a transmission rate for multicast communication in standard WiFi. To the best of our knowledge, M^3-Cast is the first work on a multi-rate and multi-channel WD multicast communication.

The key contributions of this paper are summarized as follows:

- The problem of multi-rate and multi-channel multicast communication is formulated in the context of a WD network for public safety.
- M^3-Cast protocol is proposed to select the most favourable channel for a multicast communication in a multi-channel environment. The M^3-Cast takes into account the SNR of all the operating channels on all clients present in a multicast group thereby choosing the most favourable channel for multicast communication.
- The M^3-Cast protocol chooses the most favourable transmission rate to increase reliability in a multi-rate group for multicast communication.
- The paper presents a complete system level simulations i.e., MAC and PHY layers in the context of WD for M^3-Cast protocol.
- The M^3-Cast protocol is extensively analysed in terms of multicast throughput, capacity, bit error rate (BER) for a variety of network condition such as different MIMO configurations, various bandwidths, and different network radii wherein the results are compared with the standard multicast in WD network.

III. BACKGROUND OVERVIEW AND MOTIVATION

A. GROUP FORMATION IN WD

In a WD 802.11 network, the devices that intend to communicate with each other first form a group and then exchange data with each other. In group formation, the WD protocol determines which device will act as a Group Owner (GO) and which device(s) shall join the group as client(s). In the context of WiFi alliance, a group is called a P2P group and a GO as a P2P GO. The details about the complete process of group formation can be found in [2]. Similarly, the article [20] describes the different methods of group formation as well as the L2 service discovery procedures, and the power saving mechanisms are also discussed. A client in a P2P group can be a P2P client or a legacy client.[2]

A P2P group may be a persistent P2P group (in which the GO keeps the P2P specifications of the group for future use) or a temporary P2P group (in which the specifications are not saved). Similarly, a group formation phase may be carried out either automatically or manually. In case of automatic group formation, the devices first discover each other and then initiate the process of GO negotiation which is defined in [2] in detail. On the other hand, in manual group formation, a user usually creates a group on a P2P device. In doing so the device announces itself as a GO and then invites other devices to join the group as clients. The latter kind of group formation is more popular in modern smart phones, tablets, and laptops such as WD in android [21] and Airplay or Airdrop in iOS [22]. The formation of a group may be further broken down into three phases namely: *device discovery*, *GO negotiation*, and *provisioning*. In the *device discovery* phase, the devices discover each other either by active or passive scanning. Similarly, the *GO negotiation* phase involves exchange of a GO negotiation request, GO negotiation response, and a GO confirmation message between two P2P devices. Lastly, the GO and clients exchange credentials of WiFi Protected Setup (WPS) protocol in the *provisioning* phase [2].

B. FRAME STRUCTURE IN WD

In GO negotiation phase, the devices share a Information Element (P2P IE). These IEs are little chunks of data with a numerical label which are used by management frames in order to communicate information to other systems as defined in [23]. The format of a typical P2P IE used in a WD is shown in TABLE 1.

TABLE 1. Format of P2P an information element.

Field	Size	Value	Description
IE ID	1	0xDD	IEEE 802.11 vendor specific usage
Length	1	variable	Length of P2P IE
P2P attribute	variable		Attributes of P2P IE

Furthermore, a P2P IE consists of P2P attributes to incorporate specific characteristics. A P2P attribute has a common general format that consists of a one-octet P2P attribute-ID field, a two-octet length field and a variable-length attribute-specific information field. There are certain attribute-IDs which are fixed for specific information in a P2P attribute. For example: attribute-ID 3 is used to transfer a P2P device ID;

[2] A P2P client supports both a standard WiFi and WD specification while a legacy client supports only standard WiFi.

similarly attribute-ID 11 is fixed to transfer channel lists; while attribute- ID 13 is used to send the device information of a P2P device. Similarly, attribute-IDs 19 - 220 are reserved for future use [2]. Now, a complete WD frame consists of several P2P IEs which are further made of P2P attributes as shown in Fig. 1.

FIGURE 1. Complete WD Management Frame.

C. CHANNEL AND RATE SELECTION IN STANDARD MULTICAST WD

In a WD group, the operating channel for a communication is chosen in one of two ways: (i) randomly if the group is not formed, (ii) by the GO in the case of an already formed group. In the former case, the channel is chosen in the device discovery phase in which a P2P device sends a probe request on all the social channels (i.e., available operating channels). There are three social channels i.e., 1, 6, and 11 in the case of a 2.4 GHz band. If another P2P device is interested in communication, it starts listening for a probe request on all the social channels. When a probe request is received on a certain channel, the device that receives the probe request sends a probe response to the transmitting station on that channel. This channel is then used for further communication between these devices. While in the second case, the GO is responsible for choosing a channel for a communication. The GO needs to choose a channel which is available at all other clients. If a new client wishes to join the group, it has to operate in the same channel that the GO has set for communication.

Similarly, the selection of a transmission rate for a multicast communication in a WD network is based on the multicast protocols for a standard WiFi. Thus, the multicast frames are sent at the basic transmission rate which is 6 Mb/s [2]. However, as we discussed in Section I, the protocols in the literature for example: LBP, LBP-RF, SARM, and PARF can be used to choose a multicast transmission rate.

D. MOTIVATION

The traditional channel selection procedure in a WD multicast communication is random and focuses only on the fact that the channel selection results in a channel which is common between the GO and all other clients present in a multicast group. The key benefit of this method is its simplicity, however, this simplicity comes with a cost of adverse effects on system performance. In this paper, we investigate the problem of performance degradation that may result from choosing one channel over the other in a multi-channel environment. The performance becomes more poor as the number of operating channels increases. The new IEEE standard 802.11ac operates in a 5GHz band in which there are upto 19 non-overlapping channels in the case of a 20MHz wide band channel. Thus the problem of choosing an optimal channel for a multicast communication becomes more critical.

Similarly, we are also interested in choosing an optimal transmission rate for a multi-rate environment. We also observe that the literature explores these kinds of problems from a specific perspective. It will be significantly important and useful if the problem of a multi-rate and multi-channel multicast communication is examined in the context of WD 802.11ac.

E. PUBLIC SAFETY USE CASE SCENARIOS

There are many user cases, in which the proposed protocol can be used for public safety, health, and disaster management. We present a few user cases for the sake of examples as follows.

- Information about road incidents and traffic blockage can be multicasted to vehicles so that they can change their route.
- It can also be used if a shopping mall or any other such building is in trouble and people inside the building are needed to be alarmed and guided towards safe exits.
- Similarly, another use case is an emergency situation where a person needs medical treatment or first aid immediately. There may be a doctor in the closed proximity who can help right away if we manage to inform him/her instantly.

In these, and many other cases, multicast capability of WD can be used to develop the required applications. In the following sections, first we present the proposed M^3-Cast protocol to solve this problem, and then explore M^3-Cast in depth from a system level perspective.

IV. M^3-CAST PROTOCOL

The proposed M^3-Cast protocol works in three phases namely: *Preferences Exchange*, *Preferences Outcome*, and *Data Transfer*. In *Preferences Exchange*, the clients exchange the communication channels and transmission rates that are available for multicast communication. Similarly, in *Preferences Outcome*, the GO chooses the most favourable channel and transmission rate for multicast communication. Lastly, the multicast data is sent in the *Data Transfer* phase. The detailed steps of these phases are described in Section IV-A followed by a discussions on M^3-Cast in Section IV-B.

A. OPERATION OF M^3-CAST

Phase 1: Preferences Exchange in M^3-Cast

i. Each client that is interested in the multicast communication scans all the operating channels and maintains a list of the channels (*avblCh*) that are sensed free. The channels can be scanned actively as defined in [23] or using any efficient method (for example [24] that proposes a network allocation vector (NAV)-based opportunistic prescanning process).

ii. The GO assigns a unique ID starting from 1 and incremented by 1 to each client. The GO sends

these IDs to each client at the start of the multicast communication.

iii. The GO sends a probe request to all clients in the multicast group. The probe request consists of a request for the list of the available channels (*avblCh*) at each client. The probe request also carries a general timer that defines the starting time of the probe response ($t_{startRes}$) which is sent back by each client. Each client is supposed to decode the starting time for its probe response based on its ID. A client i calculates the $t_{startRes}$ from the timing as follows:

$$t_{startRes}(i) = i \times T_{SIFS} + (i-1) \times T_{response} \quad (1)$$

where $\forall 1 \leq i \leq nClient$ while $T_{response}$ indicates the duration of the time to send the probe response from a client to the GO. We assume that $T_{response}$ is the same for all the clients. This is a reasonable assumption because first, all clients are in the same multicast group and hence they are likely to be in the close proximity of the GO. Second, the propagation delay is negligibly small due to the higher data rates and small distance. Similarly, T_{SIFS} indicates the Short Inter-Frame Space timer while *nClient* represents the total number of clients in the multicast group. An example of the timer for 3 clients is shown in Fig. 2.

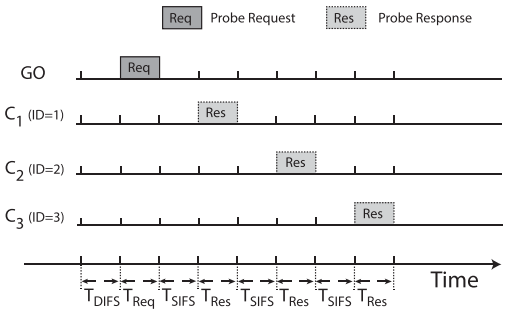

FIGURE 2. Time of probe response for three clients.

iv. Each client responds to the probe request by sending a probe response to the GO using its own $t_{startRes}$. The probe response carries a list of the available channels (*avblCh*).

v The GO selects a list of common channels (*comCh*) from the probe responses. The *comCh* is calculated in algorithm 1. If the number of common channels is one, this channel is selected for the multicast communication, otherwise phase 2 of the protocol is used to choose the most favourable channel.

Phase 2: Preferences Outcome in M^3-Cast

i. The GO sends a multicast Null Data Packet (NDP) on each channel from *commCh* pool. At the end of the NDP packet transmissions on each *commCh*, the GO informs the clients that the NDP transmission is now over.

ii. Each client calculates the SNR for each channel from the NDP frames and maintains this information in *snrMatrix*.

TABLE 2. Minimum receiver sensitivity.

MCS	Modulation	Rate (R)	Min Sens. 20MHz PPDU (dBm)	Min Sens. 40MHz PPDU (dBm)	Min Sens. 80MHz PPDU (dBm)	Min Sens. 160MHz PPDU (dBm)
0	BPSK	1/2	-82	-79	-76	-73
1	QPSK	1/2	-79	-76	-73	-70
2	QPSK	3/4	-77	-74	-71	-68
3	16-QAM	1/2	-74	-71	-68	-65
4	16-QAM	3/4	-70	-67	-64	-61
5	64-QAM	2/3	-66	-63	-60	-57
6	64-QAM	3/4	-65	-62	-59	-55
7	64-QAM	5/6	-64	-61	-58	-55
8	256-QAM	3/4	-59	-56	-53	-50
9	256-QAM	5/6	-57	-54	-51	-48

iii. Each client calculates the time for sending back the *snrChan* to the GO. The time is calculated from the timer in eq. (1). The *snrMatrix* is then sent to the GO.

iv. The GO chooses the most favourable channel (*favCh*) from the snrCh received from each client for each channel. The *favCh* is calculated as follows:

a. An SNR matrix (*snrM*) is formed from the SNR values received for all the common channels (*comCh*) from each client. The columns of the *snrM* contain the clients while the rows contain the channels.

b. For each channel (row of *snrM*), a relative cost is calculated. To do so, a minimum of the snr in each row is calculated. Then the absolute difference of the minimum form each entry in the row is calculated and finally the absolute differences are summed to get the relative cost for each channel. The cost of each channel is collected into a cost vector (*costV*).

c. The channel with the minimum in *costV* is chosen as the most favourable channel (*favCh*).

v. The GO chooses the most favourable rate (*favRate*) as follows:

a. The GO calculates the transmission rate matrix (*Rate*) that contains the transmission rate for each client for *favCh* from TABLE. 2.

b. The minimum transmission rate in the *Rate* is chosen as the most favourable transmission rate (*favRate*).

The detailed algorithm of choosing the favourite channel is given in Algorithm 2.

Phase 3: Data Transfer in M^3-Cast In this phase, the GO sends multicast data to all its clients on *favCh* communication channel with *favRate* transmission rate.

B. DISCUSSIONS ON M^3-CAST PROTOCOL

Let us discuss the different aspects of the proposed M^3-Cast protocol.

Algorithm 1 Preferences Exchange M^3-Cast

Input: $nClient$, nCh_i, $maxCh$, $avblCh$
▷ where nCh_i is the number of available channels at
▷ client i while $maxCh = \max_{1 \le i \le nClient} (nCh_i)$
▷ where $avblCh \in \mathbb{N}^{nClient \times maxCh}$
▷ The algorithm pads $maxCh - nCh_i$ zeros to nCh_i
▷ if $nCh_i < maxCh$
Output: $comCh$ ▷ where $comCh \in \mathbb{N}^{1 \times nComCh}$

$nComCh \leftarrow 0$
for $i = 1$: to $maxCh$ **do**
  $state \leftarrow 1$
  for $j = 2$ to $nClient$ **do**
    $size = length\,(avblCh\,[j]\,[maxCh])$
    for $k = 1$ to $size$ **do**
      if $avblCh[1][i] == avblCh[j][k]$ **then**
        $state \leftarrow state + 1$
      end if
    end for
  end for
  if $state == nClient$ **then**
    $nComCh \leftarrow nComCh + 1$
    $comCh[nComCh] \leftarrow avblCh[1][i]$
  end if
end for
return $comCh$

Algorithm 2 Preferences Outcome M^3-Cast

Input: $nClient$, $nComCh$, $comCh[]$, $snrM[][]$
▷ where $comCh \in \mathbb{N}^{nComCh \times 1}$
▷ and $snrM \in \mathbb{N}^{nComCh \times nClient}$
Output: $favCh$, $favRate$

$costM \leftarrow 0$ ▷ $costM \in \mathbb{N}^{nComCh \times nClient}$
$costV \leftarrow 0$ ▷ $costV \in \mathbb{N}^{nComCh \times 1}$
for $i = 1$ to $nClient$ **do**
  $max \leftarrow$ Maximum of $snrM[1{:}nComCh][i]$
  for $j = 1$ to $nComCh$ **do**
    $costM = abs(max - snrM[j][i])$
    ▷ $abs(.)$ returns the absolute value
  end for
end for
for $i = 1$ to $nComCh$ **do**
  $sum \leftarrow 0$
  for $j = 1$ to $nClient$ **do**
    $sum = snrM[i][j] + sum$
  end for
  $costV[i] = sum$
end for
$costMin \leftarrow$ Minimum of $costV[]$
$index \leftarrow i$ where $costV[i] = costMin$
$favCh \leftarrow comCh[index]$
$Rate[] \leftarrow$ transmission rate of $nClient$ for $favCh$ ▷ $Rate \in \mathbb{N}^{1 \times nClient}$
$favRate \leftarrow$ Minimum of $Rate[]$
return $favCh$ $favRate$

1) UNIQUE IDS ASSIGNMENT

The first challenge is to assign unique IDs to all clients in the multicast group. As described in Section II-B, the P2P devices use P2P attributes in Information Element to exchange the required information with each other. The attribute ID 3 is fixed for exchanging the 6 byte MAC addresses with each other. However, in addition to MAC addresses, we exploit the P2P attribute of IE for sending unique IDs to client by the GO. We use the reserved ID 19 (0x13) for this purpose and define a new P2P attribute as shown in TABLE 3. The IDs are assigned by the GO once the group is formed.

TABLE 3. Format of the proposed P2P attribute.

Field	Size	Value	Description
Attribution ID	1	0x13	Identifying the P2P attribute
Length	2	variable	Length of P2P attribute
Client ID	variable		Unique ID assigned to a client

2) A NEW CLIENT JOINS/LEAVES

We describe the required procedure if a new client joins or leaves the multicast group. In the case where a new client joins the multicast group, the GO assigns it the next possible ID. We assume that there are three clients i.e., C_1, C_2, and C_3 with IDs 1,2 and 3, respectively in the group. When a new client, say C_4 joins the group, it is assigned an ID=4. On the other hand, if a client leaves the multicast group, the GO assigns the ID of the leaving client to the client with the highest ID. Suppose C_2 leaves the group, then the GO changes the ID of C_4 only and assigns it the ID=2 instead of reshuffling the IDs of all clients in the group. If two clients leave the group, then the clients with highest and 2nd highest IDs are assigned the IDs of the leaving clients. If a client with the highest ID leave the group, then there is no need for changing the IDs of the existing members.

V. ANALYTICAL MODEL

In this section, an analytical model is formulated to evaluate the theoretical performance of M^3-Cast protocol in terms of multicast throughput, capacity and BER.

A. SYSTEM MODEL

Let there be a GO and N_{client} clients in a multicast group. Let $N_{H,i}$ and N_H indicate the total number of available channels at client i and the total number of common channels at GO, respectively. Let $H_{com} \in \mathbb{N}^{N_H \times 1}$ show the common channels at GO while $Cl \in \mathbb{N}^{1 \times N_{clients}}$ indicate the N_{client} clients in the

multicast group as shown in eq. (2).

$$H_{com} = \begin{bmatrix} 1 \\ 2 \\ \vdots \\ N_H \end{bmatrix}, \qquad Cl = \begin{bmatrix} 1 & 2 & \dots & N_{client} \end{bmatrix} \tag{2}$$

Let $\Omega \in \mathbb{R}^{N_H \times N_{client}}$ represent the SNR values of all common channels for each client. Without the loss of generality, let $R \in \mathbb{R}^{N_H \times N_{client}}$ show the transmission rate for N_H common channels for N_{client} clients. Let ω_{ij} indicate an element of Ω that represents the SNR of channel i for client j. The elements of the Ω are illustrated in eq. (3).

$$\Omega = \begin{bmatrix} \omega_{11} & \omega_{12} & \dots & \omega_{1N_{client}} \\ \omega_{21} & \omega_{22} & \dots & \omega_{2N_{client}} \\ \vdots & \vdots & \ddots & \vdots \\ \omega_{N_H 1} & \omega_{N_H 2} & \dots & \omega_{N_H N_{client}} \end{bmatrix} \tag{3}$$

The probability distribution of the Ω is discussed in Section V-F. Let r_{ij} indicate an element of R that represent the transmission rate of client j for channel i as shown in eq. (4).

$$R = \begin{bmatrix} r_{11} & r_{12} & \dots & r_{1N_{client}} \\ r_{21} & r_{22} & \dots & r_{2N_{client}} \\ \vdots & \vdots & \ddots & \vdots \\ r_{N_H 1} & r_{N_H 2} & \dots & r_{N_H N_{client}} \end{bmatrix} \tag{4}$$

where the transmission rate r_{ij} is determined based on SNR value ω_{ij} as discussed later on and illustrated in TABLE 2.

Let $\Delta \in \mathbb{R}^{N_H \times N_{client}}$ illustrate the relative cost matrix corresponding to each channel for every client as shown in eq. (5).

$$\Delta = \begin{bmatrix} \delta_{11} & \delta_{12} & \dots & \delta_{1N_{client}} \\ \delta_{21} & \delta_{22} & \dots & \delta_{2N_{client}} \\ \vdots & \vdots & \ddots & \vdots \\ \delta_{N_H 1} & \delta_{N_H 2} & \dots & \delta_{N_H N_{client}} \end{bmatrix} \tag{5}$$

where the element δ_{ij} is calculated in eq. (6).

$$\delta_{ij} = abs\Big(\max_{1 \le k \le N_H} (\omega_{kj}) - \omega_{ij} \Big) \tag{6}$$

where the function $abs(.)$ calculates the absolute value. Let $\Psi \in \mathbb{R}^{N_H \times 1}$ represent the relative cost of each channel. The element ψ_i of the vector ψ indicates the cost of channel i as shown in eq. (7).

$$\Psi = \begin{bmatrix} \psi_1 \\ \psi_2 \\ \vdots \\ \psi_{N_H} \end{bmatrix} \tag{7}$$

where element ψ_i for a channel i is calculated in eq. (8).

$$\psi_i = \sum_{j=1}^{N_{client}} \delta_{ij} \tag{8}$$

B. MOST FAVOURABLE COMMUNICATION CHANNEL SELECTION FOR M³-CAST

At this point, we have a relative cost for each common channel at GO. Let f be an injective function that maps the cost vector Ψ to the common channels vector H_{com} as shown in eq. (9).

$$f : \Psi \rightarrow H_{com} \tag{9}$$

Then the most favourable channel (θ) can be calculated in eq. (10).

$$\theta = f\Big(\min_{1 \le i \le N_H} (\psi_i) \Big) \tag{10}$$

Thus the SNR values for the optimal channel $\theta \in \mathbb{N}^{N_H \times 1}$ are given by the vector Ω_θ where $\Omega_\theta \subset \Omega$ for N_C clients as shown in eq. (11).

$$\Omega_\theta = \begin{bmatrix} \omega_{\theta 1} & \omega_{\theta 2} & \dots & \omega_{\theta N_{client}} \end{bmatrix} \tag{11}$$

The element $\omega_{\theta i}$ indicates the SNR value of the optimal channel for client i.

C. MOST FAVOURABLE TRANSMISSION RATE SELECTION FOR M³-CAST

Let R_θ where $R_\theta \subset R$ indicate the transmission rates of N_{client} clients for the most favourable channel θ as shown in eq. (12).

$$R_\theta = \begin{bmatrix} r_{\theta 1} & r_{\theta 2} & \dots & r_{\theta N_{client}} \end{bmatrix} \tag{12}$$

The GO chooses the minimum transmission rate as the most favourable transmission rate $r_{optimal}$ in order to make the transmission reliable for the client with the worst channel condition as shown in eq. (13).

$$r_{fav} = \min_{1 \le i \le N_H} \big(r_{\theta i} \big) \tag{13}$$

The GO informs the clients about the most favourable channel and rate in a multicast message. The clients listen to the multicast transmission on the most favourable channel.

D. BIT ERROR RATE CALCULATION

Let BER_i indicate the BER of a client i, then an expression can be derived for BER_i based on $\omega_{\theta i}$. There are two main methods to calculate BER from a given SNR. One method is based on standard formula [27] that takes into account the SNR value, and data rate which in return can be calculated from given modulation and coding schemes. The second method uses empirical curves for a specific vendor to calculate BER from a given SNR value [28].

In order to calculate BER_i using the first method, let γ_i and B_i denote the E_b/N_o i.e., the energy per bit and bandwidth of the given channel, respectively for a client i. Then γ_i is calculated as shown in eq. (14).

$$\gamma_i = \frac{B \times 10^{\omega_{\theta i}/10}}{r_{fav}} \tag{14}$$

BER_i can be derived as a function of γ_i and MCS which indicates the modulation and coding scheme used by GO as shown in eq. (15).

$$BER_i = f(\gamma_i, MCS) \tag{15}$$

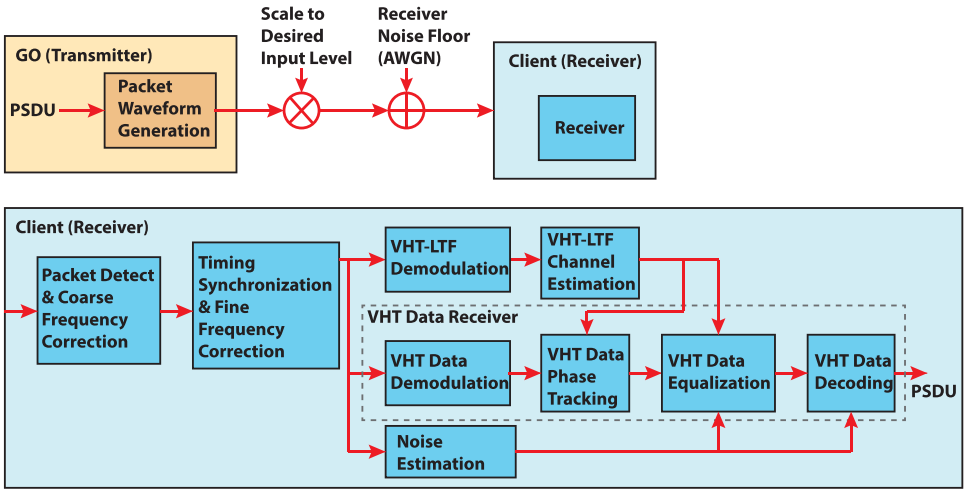

FIGURE 3. Simulation System Model.

A complete list of formula for BER for different MCS can be found in [27].
Conversely, BER for different SNR can be calculated from empirical curves as discussed in [28].

Let $P_{e,i}$ denote the probability of channel error for a client i as listed in eq. (16).

$$P_{e,i} = 1 - (1 - BER_i)^L \tag{16}$$

where L is the packet length in bits.

E. MULTICAST THROUGHPUT OF M^3-CAST

The throughput S_i is the number of successful bits transmitted in a unit time to client i from the GO. In order to estimate the total multicast throughput S at GO, the individual throughput from GO to each client is calculated. For this purpose, the throughput from GO to a client i in the multicast group is formulated. Thus the multicast throughput S is calculated in eq. (17).

$$S = \frac{1}{N_C} \sum_{n=1}^{N_C} S_n \tag{17}$$

We calculate the throughput S_i as the number of total bits successfully transmitted in a single frame per the total time T for a single frame including the overhead as shown in eq. (18).

$$S_i = \frac{1 - P_{e,i}}{T} \tag{18}$$

where the total time T is calculated in Appendix A. It is assumed that T is same for all the clients in the multicast group. See Appendix A for a detailed calculation of T.

F. CALCULATION OF SNR VALUES

In this subsection, the probability distribution of the SNR values in Ω is discussed. Let the element ω_{ij} of the matrix Ω be represented by a random variable X. An element ω_{ij} of the Ω for a channel i of a client j can be modelled by a log normal distribution. Then X can be defined in eq. (19).

$$X = E + W \tag{19}$$

where E and W indicate the RSS (Received Signal Strength) and the noise floor, respectively. E and W in eq. 19 are expressed in logarithmic scales i.e., (dBm). The noise floor W depends on many factors in the environment. However, its value can be be approximately measured using eq. (20) while E is calculated in eq. (21) [27].

$$W = 10 \times log_{10}(k \times T \times F_s) + NF \tag{20}$$

where T indicates the ambient temperature in $Kelvin(K)$, k is the Boltman's constant ($k = 1.3806 \times 10^{-23} J/K$), F_s indicates the sampling frequency in Hz which is equal to the channel's bandwidth, while NF indicates the noise factor of the system's hardware.

$$E = P_t - PL(d) \tag{21}$$

where P_t indicates the power of the transmitter in dBm. Its value depends on the standard and vendor's implementation. Similarly, the $PL(d)$ indicates the Path Loss in dBm at a distance d (m) between transmitter and receiver. $PL(d)$ is calculated in eq. (22).

$$PL(d) = \begin{cases} PL_{FS}(d) + \chi_\sigma & \text{i} \\ PL_{FS}(d_{BP}) + 3.5 \times 10 log_{10}(\frac{d}{d_{BP}}) + \chi_\sigma & \text{ii} \end{cases} \tag{22}$$

where eq. (22-i) holds if $d \leq d_{BP}$ and eq. (22-ii) holds if $d > d_{BP}$. Similarly, d_{BP} in eq. (22) indicates the breakpoint distance in (m) while $PL_{FS}(.)$ refers to the free space path loss in dB. Similarly, χ_σ shows a Guassian random variable with zero mean, i.e., $\mu = 0$ and with standard deviation of σ i.e., $\chi_\sigma \sim ln\mathcal{N}(\mu, \sigma^2)$. It is used to model the log normal shadowing in the path loss. The $PL_{FS}(.)$ is calculated in eq. 23 while the Probability Distribution Function (PDF)

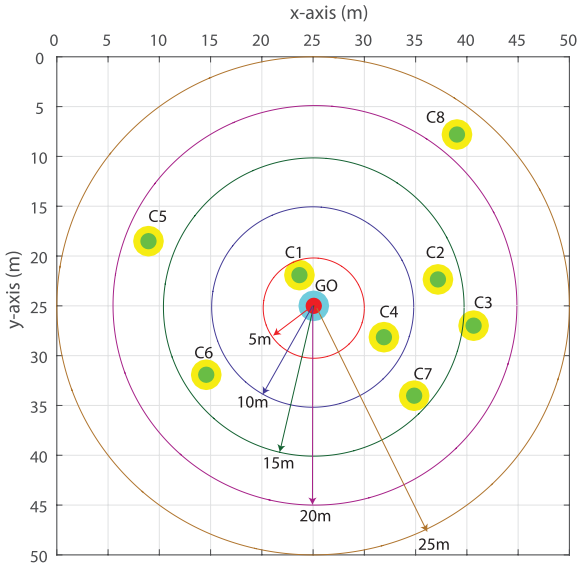

FIGURE 4. Network Architecture.

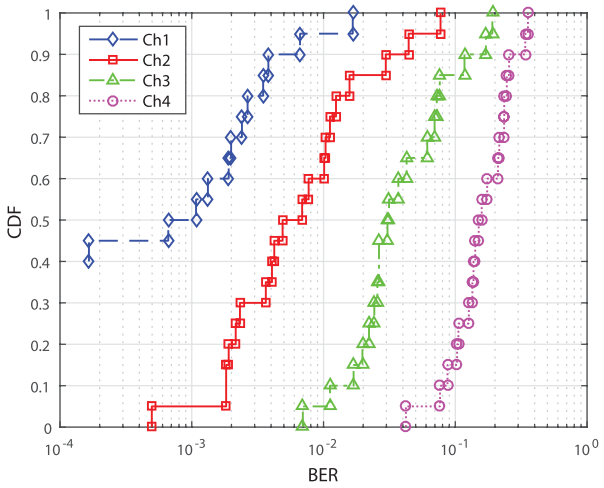

FIGURE 5. BER of four different channels.

of the Guassian random variable χ_σ with zero mean ($\mu = 0$) and the standard deviation σ of the χ_σ is given in eq. (24).

$$PL_{FS}(d) = -10 \times log_{10}\left(\frac{G_t G_r \lambda^2}{(4\pi d)^2}\right) \tag{23}$$

where G_t and G_r indicate the transmitter and receiver antenna gains, respectively, d is the distance between transmitter and receiver in meters, and λ indicates the wavelength of the transmitted signal in meters.

$$P(\chi_\sigma) = \frac{1}{\sqrt{2\pi}\sigma} \times \exp^{\left(-\frac{\chi^2}{2\sigma^2}\right)} \tag{24}$$

G. MULTICAST CHANNEL CAPACITY OF M3-CAST

We may subsequently derive the channel capacity (C_{ij}) of a channel i for a client j using the information of SNR values (ω_{ij}) and a channel matrix H_{ij} where H_{ij} represents the

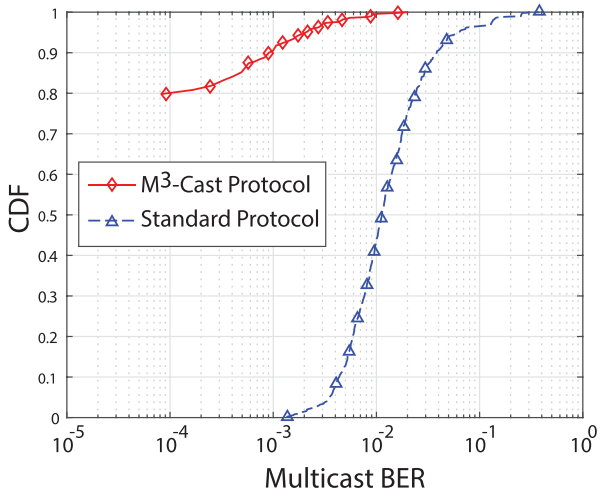

FIGURE 6. BER of the proposed method and standard method.

narrowband time-invariant wireless channel i for a client j. Let N_R and N_T represents the number of transmitter and receiver antennas, respectively then $H_{ij} \in \mathbb{C}^{N_R \times N_T}$. We assume that each transmitter sends an independent steams of input symbols $x \in \mathbb{C}^{N_T \times 1}$ with power E_x such that the total transmitted power is $P_t = N_T \times E_x$. Then, the received symbols' $y \in \mathbb{C}^{N_R \times 1}$ for a channel i and client j can be written in a matrix form as shown in eq. (25).

$$y = H_{ij}x + n_{ij} \tag{25}$$

where n_{ij} represents the noise vector of channel i at client j. We assume that the noise is iid i.e., independent and identically distributed with zero mean and variance of σ^2. Thus the auto-correlation matrix is $R_{nn} = \sigma^2 I$ where I is an $N_R \times N_T$ identity matrix.

The Shannon capacity Cij for this stationary channel i for client j can be written as [29].

$$C_{ij} = log_2\left[det\left(I + \frac{E_x}{\sigma^2} H_{ij} H_{ij}^{\dagger}\right)\right] \tag{26}$$

where $H_{ij}^{\dagger}$ indicates the Hermitian or the complex conjugate transpose of the channel matrix H_{ij}. Note that the eq. (25) gives the capacity of the channel in bits per sec (bps)/Hz.

In order to calculate the ergodic capacity $\overline{C_{ij}}$ of the channel C_{ij}, S realization of the channel matrix H_{ij} are considered. Thus $\overline{C_{ij}}$ becomes the expected value of the stationary capacity [29]. Eq. (27) is used to calculate the $\overline{C_{ij}}$.

$$\overline{C_{ij}} = E_S[C_{ij}] = E_S\left[log_2\left\{det\left(I + \frac{E_x}{\sigma^2} H_{ij} H_{ij}^{\dagger}\right)\right\}\right] \tag{27}$$

VI. RESULTS AND DISCUSSIONS

A. SIMULATION SETUP

The simulation setup is defined in this section. In order to evaluate the performance of the M3-Cast protocol, a detailed system is implemented in matlab as shown in Fig. 3. The model is based on the architecture of 802.11ac physical layer [8] and TGn channel 802.11 [26]. TABLE. 2 illustrates

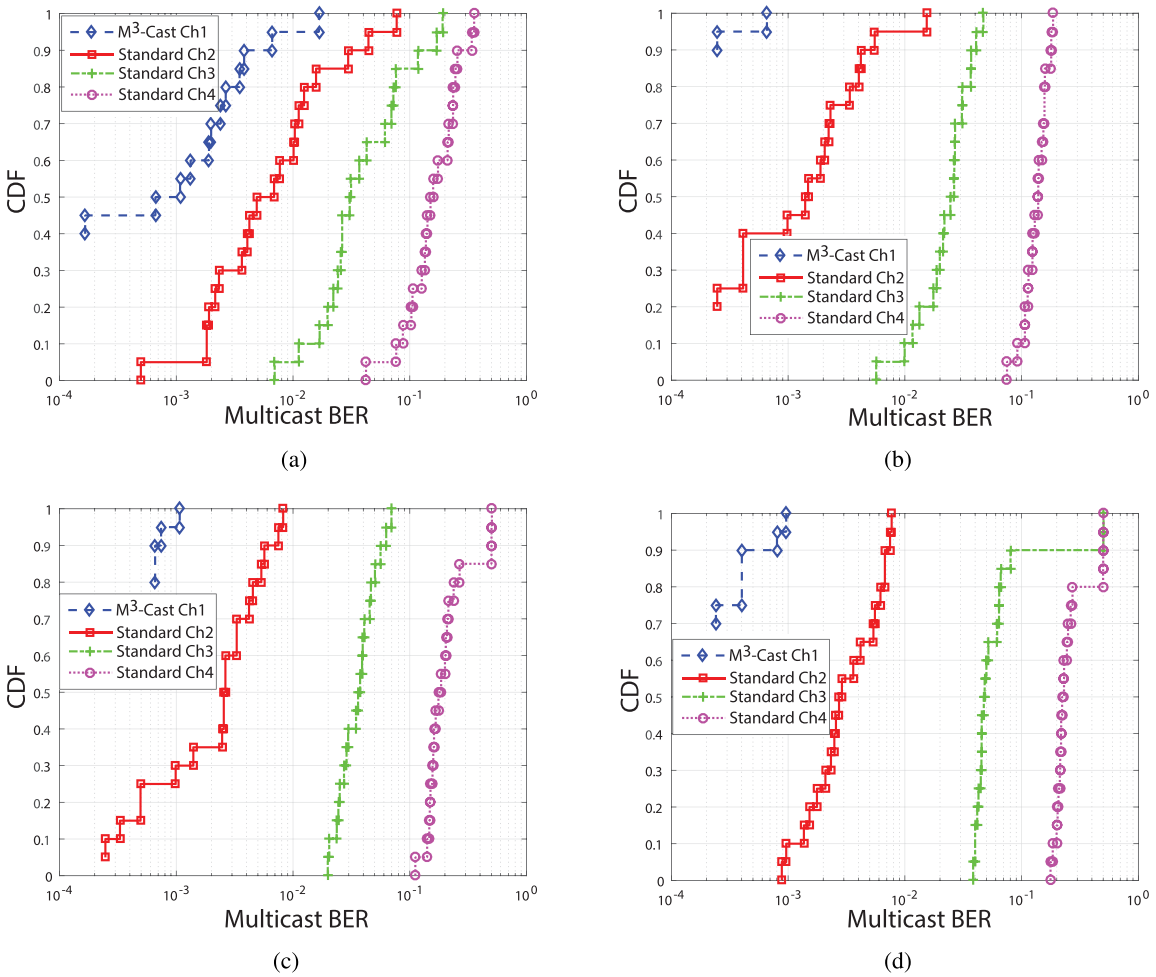

FIGURE 7. CDF of Multicast BER for SISO and different MIMO configurations. (a) 1×1 SISO. (b) 2×2 MIMO. (c) 4×4 MIMO. (d) 8×8 MIMO

the minimum sensitivity level for different modulations and coding schemes (MCS) and different channel bandwidths.

B. NETWORK ARCHITECTURE

A general network scenario has been created to evaluate the performance of M^3-Cast protocol. There is one GO and k clients in a multicast group in a 2-D coordinate system of 50x50 m^2 area. As shown in Fig. 4, the GO is situated in the centre of this area, i.e. at coordinates (25,25), and the clients are randomly deployed around GO in a circle where the radius varies from 1m to 25m based on the chosen MCS. This is because we consider isotropic transmit antenna(s) with unity gains at GO. Thus a circular region of radius 1-25m around GO is considered as the transmission region of GO. The motive behind choosing a minimum of 1m distance is to avoid any near field communication losses, while a maximum of 25m is to avoid the total loss of signals.

C. IMPACT OF SNR ON CHANNEL

First of all we investigate the impact of selecting a channel with different SNR on the performance of the system in terms of BER. For this purpose, we consider four common channels namely: Ch1, Ch2, Ch3, and Ch4 available for a multicast communication between the GO and five clients. The GO can choose any channel and start transmission to its clients. To this end, the GO chooses a 20MHz channel bandwidth with MCS=2 i.e., QPSK modulation and a coding rate of 3/4. Thus the minimum sensitivity level at the clients is -77 dBm as illustrated in TABLE. 2. Due to the random nature of the wireless medium, it is reasonably possible that each channel may add different noise and interference to the transmitted signal when it reaches any specific client. For the sake of argument, let us examine the SNR at each channel at a certain client. The relationship between SNR and distance d can be found in Appendix B. We further proceed by carefully choosing d, such that the transmitted signal is received -9 dBm, -10 dBm, -11 dBm, and -12 dBm below the minimum sensitivity level (-77 dBm) at channels Ch1, Ch2, Ch3, and Ch4, respectively. The receive noise floor is set to -95dBm in this case. The packet length is 1500 bytes while SISO is used. Thus using eq. (19), the final SNR values of each channel is shown in TABLE. 4. The purpose of this

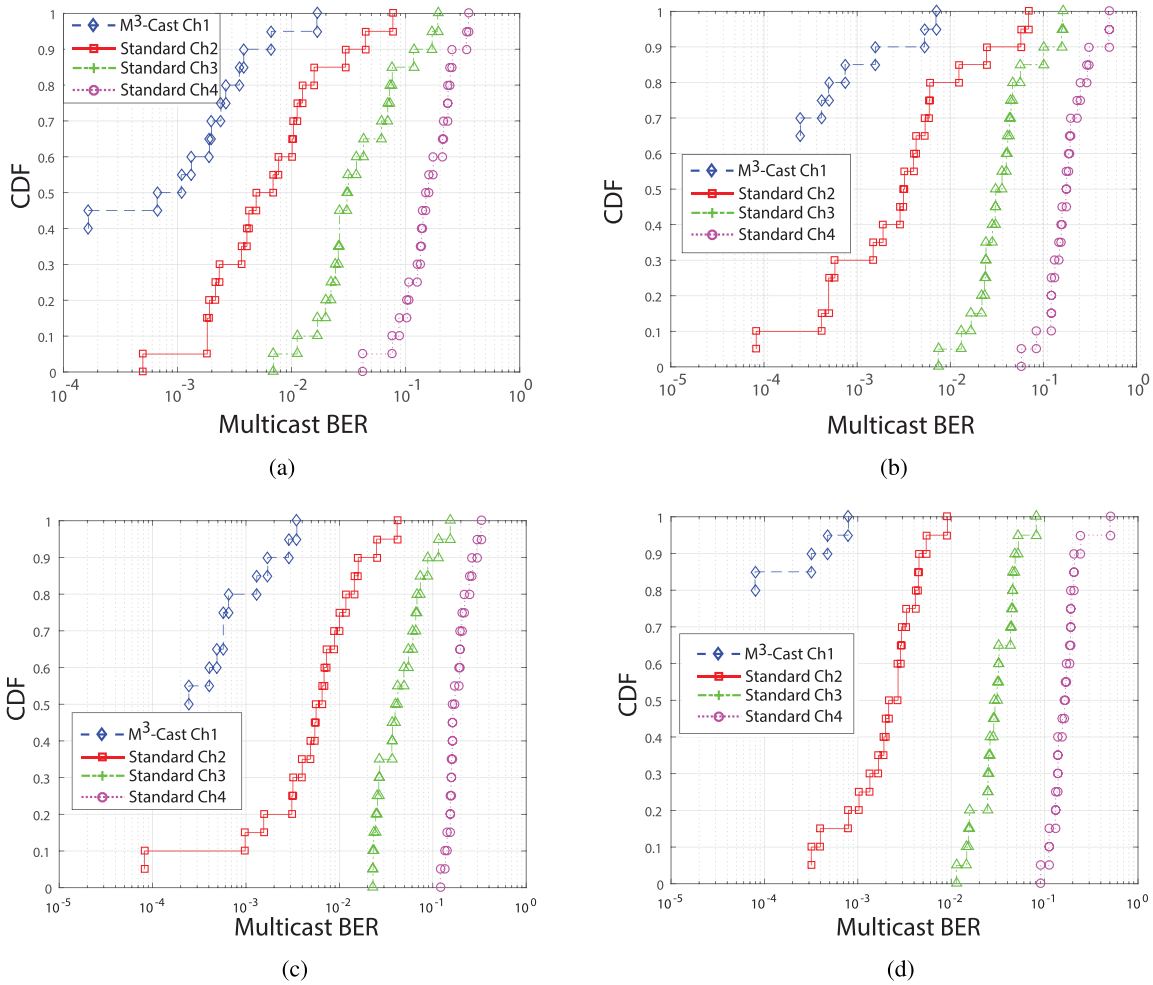

FIGURE 8. CDF of multicast BER for different channel bandwidths. (a) 20 MHz channel. (b) 40 MHz channel. (c) 80 MHz channel. (d) 160 MHz channel.

TABLE 4. The RSS and SNR values of the four channels at the receiver.

Channel	RSS (dBm)	SNR (dB)
Ch1	-86	9
Ch2	-87	8
Ch3	-88	7
Ch4	-89	6

experiment is to assess the loss in terms of BER when the SNR of a channel changes by 1 dB. The BER of each channel is shown in the Fig. 5.

We observe that the change of SNR over 1 dB can have greater impact on the distribution of BER. As shown in Fig. 5, almost 95% of BER for Ch1 is below 0.01, while almost 30% of BER for Ch2 is between 0.1 and 0.01. Similarly, around 85% BER lies between 0.1 and 0.01 interval for Ch3. Lastly approximately 85% of BER is above 0.1 for Ch4. Thus as the SNR value decreases over 1 dB, the BER increases by almost 10%.

Next, we examine the BER of the above four channels using M^3-Cast protocol and the standard method. With standard protocol, the GO can select any of the four channels with equal probability, while with the M^3-Cast protocol, the GO selects the best possible channel. As shown in Fig. 6, almost 98% of BER is below 0.01 in the case of M^3-Cast protocol. On the other hand, around 60% of BER is above 0.01 and 5% of BER is even greater than 0.1 in the case of the standard protocol.

D. IMPACT OF MIMO CONFIGURATIONS

In order to asses the effects of Single Input Single Output (SISO) and different MIMO configurations on M^3-Cast protocol, we calculate the multicast BER for four different channels with different SNR values as illustrated in Table 4. The results under a SISO and different MIMO configurations (i.e., 2×2, 4×4, and 8×8) are shown in Fig. 7a-7d in terms of Cumulative Distribution Function (CDF) vs. BER. We notice that the BER increases as we increase the number of transmitter and receiver antennas for all MIMO configurations for all four channels. However, the multicast BER for

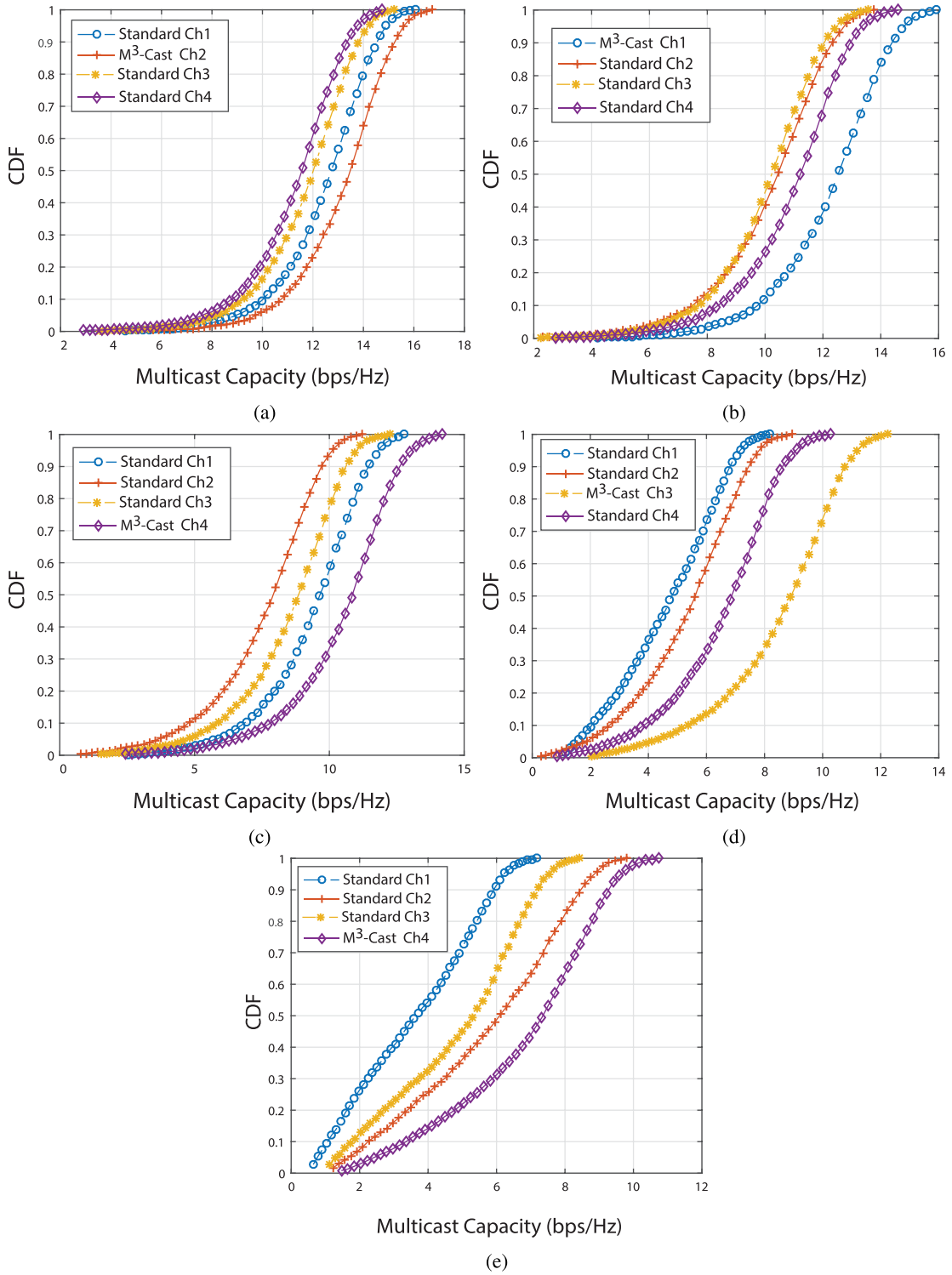

FIGURE 9. **Multicast Capacity for a Network of radius 5m,10m,15m,20m {7 Clients | 4 Channels}. (a) Network of radius 5m. (b) Network of radius 10m. (c) Network of radius 15m. (d) Network of radius 20m. (e) Network of radius 25m.**

the channel chosen by M^3-Cast is less than that of the standard protocol. As shown in Fig. 7a, almost 84%, 95%, and 100% of BER is above 0.1 for SISO, 2×2 and 4×4 MIMO configurations in the case of Ch4 using standard protocol. Similarly, 20% of BER is above 0.5 for 8×8 MIMO when Ch4 is chosen by standard protocol. On the other hand, 50% BER for SISO and 100% of BER in the case of 2×2, 4×4, and 8×8 MIMO configuration is under 0.001 when the proposed method is

used. Hence, M^3-Cast protocol tremendously reduces the multicast BER as compared to the standard method for SISI and all MIMO configurations in WD.

E. IMPACT OF CHANNEL BANDWIDTH

Next we examine the impact of different channel bandwidths on the performance of a multicast communication in terms of BER for our four representative channels. As shown in Fig. 8a-8d, the overall BER increases as we increase the channel bandwidth. However, the BER of the proposed method is substantially smaller as compared to the standard method. For example, 90%, 95%, 100%, and 100% BER are greater than 0.01 for 20MHz, 40MHz, 80MHz, and 160MHz bandwidths respectively, when a standard protocol is used. On the contrary, 50%, 80%, 80%, and 100% BER is less than 0.001 with M^3-Cast protocol. Thus the M^3-Cast protocol surpasses the standard method for different channel bandwidths.

F. MULTICAST CHANNEL CAPACITY

In this section, we examine the numerical multicast channel capacity of M^3-Cast protocol and the standard protocol as derived in Section. IV. The multicast channel capacity can vary for different network parameters. Thus in order to reflect the validity of the proposed method for different network parameters, we calculate the channel capacity for different network radii i.e., 5m, 10m, 15m, 20m, and 25m. As shown in Fig. 4, we consider one GO and choose seven multicast clients. The clients are randomly distributed around the GO for a given network radius. Fig. 9a-9e show the multicast capacity of four channels for different network radii. We observe the multicast capacity decreases as we increase the radius of the network. This is because increasing the network size results in increasing the probability of lower SNR due to greater distance. However, M^3-Cast protocol increases the multicast capacity as compared to the standard method for all network sizes.

We also calculate the average multicast capacity for different network sizes both for M^3-Cast and standard algorithm as shown in Fig.10. It can be seen that in the case of 1m to 5m network radius, the average multicast capacity of M^3-Cast is 11.19bps/Hz (Ch2) while it is 10.32bps/Hz (Ch1), 9.39bps/Hz (Ch3), and 8.83bps/Hz (Ch4) for standard method. Thus the capacity gain by M^3-Cast is 17.65% for a network of radius 5m. Similarly, M^3-Cast achieves a capacity gain of 20.64%, 21.43%, 44.02%, and 28.85% for network of radii 10m, 15m, 20m, and 25m, respectively as compared to average multicast capacity of the standard method. Hence M^3-Cast outperforms the standard method in terms of multicast capacity for different network sizes.

G. MULTICAST THROUGHPUT

In order to assess the performance of M^3-Cast protocol from a system perspective i.e., (MAC and PHY layers), we calculate the multicast throughput from our theoretical model derived

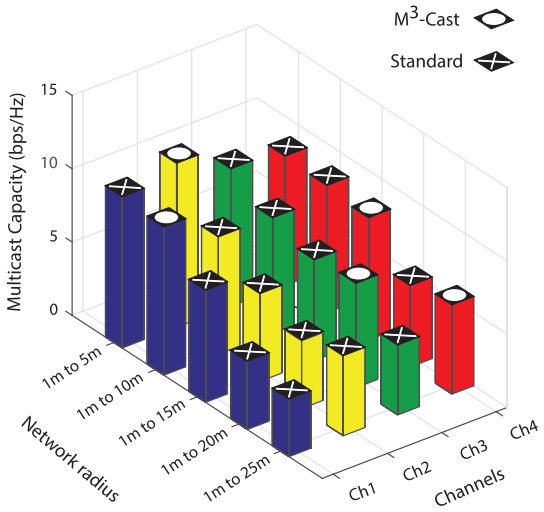

FIGURE 10. Average multicast capacity for network of radius 5m, 10m,15m, 20m, 25m {7 Clients | 4 Channels}.

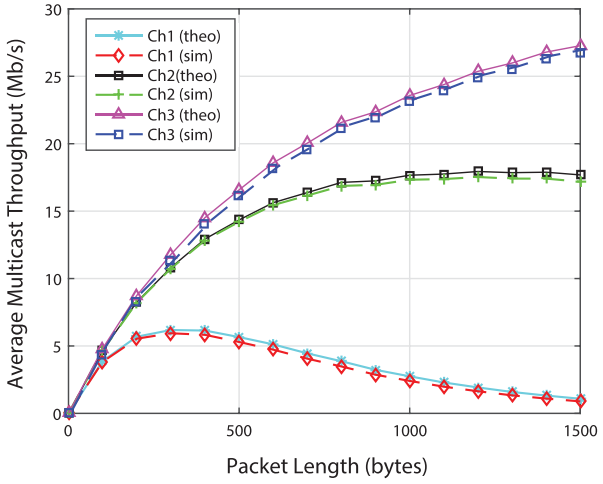

FIGURE 11. Average multicast throughput for different channels.

in Section. IV and simulation model shown in Fig. 3. For this purpose, we deploy five clients around GO with three common channels namely Ch1, Ch2, and Ch3 among all clients such that the SNR of each channel is different than others by at least 1dB. We use 20MHz bandwidth with 16-QAM under TGn channel C with parameters shown in TABLE 7. The theoretical multicast throughput is calculated from eq. (17) in Section V-E. TABLE 5 lists the parameters used in eq. (17) and APPENDIX A to calculate the multicast throughput. The theoretical (theo) and simulation (sim) average multicast throughput for Ch1, Ch2, and Ch3 are illustrated in Fig. 11. As we increase the packet length at MAC layer, average multicast theoretical and simulation throughput increases for all the three common channels. However, each channel gives a different throughput. Next, we calculate the average multicast throughput for the standard and M^3-Cast protocols as shown in Fiq. 12. The simulation results in Fig.12 indicates that M^3-Cast improves the average multicast

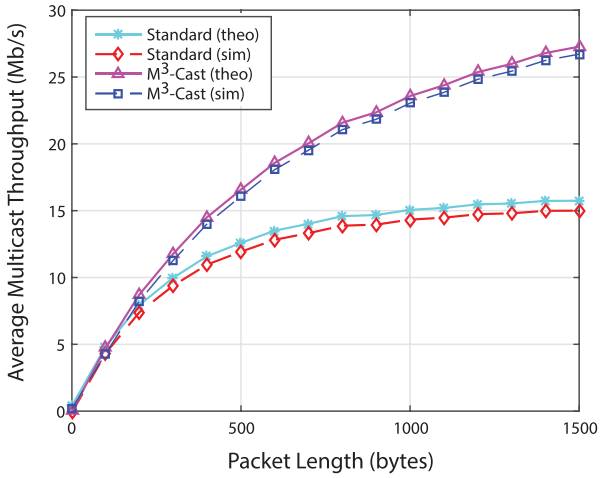

FIGURE 12. Average multicast throughput of the proposed and standard methods.

throughput by almost 38% i.e., from about 12.02Mb/s to 16.6Mb/s as compared to standard method when the packet length is 500 bytes. The throughput gain rises tremendously as we increase the packet size. For example, M^3-Cast achieves 23.5Mb/s throughput for a packet size of 1000 bytes whereas the standard algorithm achieves 14.2Mb/s for the same packet size. The improvement is 65% in this case. Similarly, for a packet size of 1500 bytes, M^3-Cast almost doubled the average multicast throughput. The theoretical results confirm the simulation results.

VII. CONCLUSION

This paper proposed that M^3-Cast protocol is more effective than the standard multicast protocol because it chooses the most favourable communication channel and transmission rate for a multi-channel and multi-rate multicast communication in the context of public safety using a WD 802.11ac network. M^3-Cast was evaluated by a theoretical formulation as well as tested on a complete system level simulation model that implements the MAC and PHY layers of a WD 802.11ac system. The simulation and theoretical results show that the M^3-Cast protocol surpasses the standard method by almost two times in terms of multicast throughput, capacity, and BER under different MIMO configurations, various channel bandwidths, and different network sizes. In future work, M^3-Cast protocol can be extended for a hidden node problem and interference due to other wireless networks operating in the same band.

APPENDIX A

The total time T is calculated in eq. (A.1).

$$T = T_{DIFS} + T_x \tag{A.1}$$

where T_{DIFS} and T_x indicate the DCF Inter-Frame Spacing time, and the transmission time of the multicast frame, respectively. The T_{DIFS} is illustrated in TABLE. 5 whereas

TABLE 5. MAC and PHY Parameters.

Parameter	Value	Para	Value	Para	Value
Slot time (σ)	9 μs	CW_{min}	16	T_{DIFS}	34 μs
L_{macH}	34 bits	CW_{max}	1024	T_{SIFS}	16 μs
$T_{VHT-STF}$	4 μs	T_{SYMS}	3.6 μs	T_{STF}	8 μs
$T_{VHT-SIG-A}$	8 μs	T_{L-SIG}	4 μs	T_{LTF}	8 μs
$T_{VHT-SIG-B}$	4 μs	T_{SYML}	4 μs	N_{tail}	6 bits
$T_{VHT-LTF}$	4 μs	$N_{service}$	16 bits	ρ	1 μs

TABLE 6. Parameters of VHT PPDU.

Parameter	Details
T_{L-STF}	Transmission time of Legacy Short Training Field
T_{L-LTF}	Transmission time of Legacy Long Training Field
T_{L-SIG}	Transmission time of Legacy Signal field
$T_{VHT-SIG-A}$	Transmission time of Very High Throughput-Signal A field
$T_{VHT-STF}$	Transmission time of Very High Throughput Short Training Field
$T_{VHT-LTF}$	Transmission time of Very High Throughput Long Training Field
$T_{VHT-SIG-B}$	Transmission time of Very High Throughput-Signal B field

T_x is derived in eq. (A.2).

$$\begin{aligned} T_x &= T_{LEG-PREAMBLE} + T_{L-SIG} \\ &\quad + T_{VHT-SIG-A} + T_{VHT-PREAMBLE} \\ &\quad + T_{VHT-SIG-B} + T_{DATA} \end{aligned} \tag{A.2}$$

$$T_{LEG-PREAMBLE} = T_{L-STF} + T_{L-LTF} \tag{A.3}$$

$$T_{VHT-PREAMBLE} = T_{VHT-STF} + N_{VHTLTF} \times T_{VHT-LTF} \tag{A.4}$$

where T_{L-STF}, T_{L-LTF}, T_{L-SIG}, $T_{VHT-SIG-A}$, $T_{VHT-STF}$, $T_{VHT-LTF}$, and $T_{VHT-SIG-B}$, indicate the transmission times of different fields of a VHT-PPDU frame as illustrated in TABLE 6. The N_{VHTLTF} indicates the number of long training symbols which is determined from the number of space-time streams [27]; while T_{DATA} represents the transmission time of data which is calculated in eq. (A.7).

Similarly, T_{STF} and T_{LTF} are calculated in eq. (A.5) and eq. (A.6), respectively.

$$T_{STF} = 10\left(\frac{T_{FFT}}{4}\right) \tag{A.5}$$

where $T_{FFT} = 1/\triangle F$ while $\triangle F$ indicates the subcarrier frequency spacing in kHz. For a 20MHz channel bandwidth under OFDM, the $\triangle F = 312.5$ kHz. Thus $T_{FFT} = 3.12$ μs and $T_{SHORT} = 8$ μs. It can also be calculated for a 40MHz channel bandwidth and other channel bandwidths [8].

$$T_{LTF} = 2.T_{FFT} + T_{GI2} \tag{A.6}$$

By using T_{GI2} and T_{FFT} in Eq. (A.6), the $T_{LTF} = 8$ μs.

$$T_{DATA} = \begin{cases} N_{SYM} \times T_{SYM} & \text{for long GI} \\ T_{SYML}\lceil \frac{T_{SYMS} \times N_{SYM}}{T_{SYML}} \rceil & \text{for short GI} \end{cases} \tag{A.7}$$

TABLE 7. TGn channel profile models.

Channel Model	Details
A	A typical office environment with NLOS conditions and $\sigma_{RMS} = 0ns$ (Optional)
B	A typical large open space and office environments, NLOS conditions with $\sigma_{RMS} = 15ns$
C	A large open space (indoor and outdoor) NLOS conditions with $\sigma_{RMS} = 30ns$
D	A large open space (indoor and outdoor) LOS conditions with $\sigma_{RMS} = 50ns$
E	A large open space (indoor and outdoor) LOS conditions with $\sigma_{RMS} = 100ns$
F	A large open space (indoor and outdoor) LOS conditions with $\sigma_{RMS} = 150ns$

where GI, T_{SYM}, T_{SYMS} and T_{SYML} indicate Guard Interval, symbol interval, short GI symbol interval, and long GI symbol interval, respectively. Their values are listed in TABLE 5.

$$T_{SYM} = \begin{cases} T_{SYML} & \text{for long GI} \\ T_{SYMS} & \text{for short GI} \end{cases} \tag{A.8}$$

$$N_{SYM} = m_{STBC} \times \lceil \frac{M}{m_{STBC} \times N_{DBPSL}} \rceil \tag{A.9}$$

where $\lceil x \rceil$ = smallest integer $\geq x$ and N_{DBMS} indicates the number of data bits per symbol.

$$M = 8 \times APEP_{LENGTH} + N_{Service} + N_{tail} \times N_{ES} \tag{A.10}$$

$$m_{STBC} = \begin{cases} 2 & \text{if STBC is used} \\ 1 & \text{otherwise} \end{cases} \tag{A.11}$$

where $APEP_{LENGTH}$ indicates the final value of A-MPDU i.e., payload size and N_{ES} represents the number of Binary Convolution Code (BCC) encoders. The value of N_{ES} depends on the MCS and channel bandwidth and their details can be found in [8]. Space-Time Block Coding (STBC) is an encoding technique that greatly improves the reliability of communication in 802.11ac. T_x is calculated by using eq. (A.3-A.8) in eq. (A.2).

APPENDIX B

The equations derived for SNR values in the eq. (19-23) show that calculation of SNR values depends on different path loss parameters. In order to model the channel for 802.11 in different environments, a set of six profiles namely TGn channel models A-F as illustrated in TABLE 7 is proposed in [26]. Each profile represents a different environment with specific Root Mean Square (RMS) delay spread (σ_{RMS}), standard deviation (σ) and Line-Of-Sight (LOS)/Non-Line-Of-Sight (NLOS) conditions, as illustrated in TABEL 8. More detials on channel profiles for 802.11 can be found in [26].

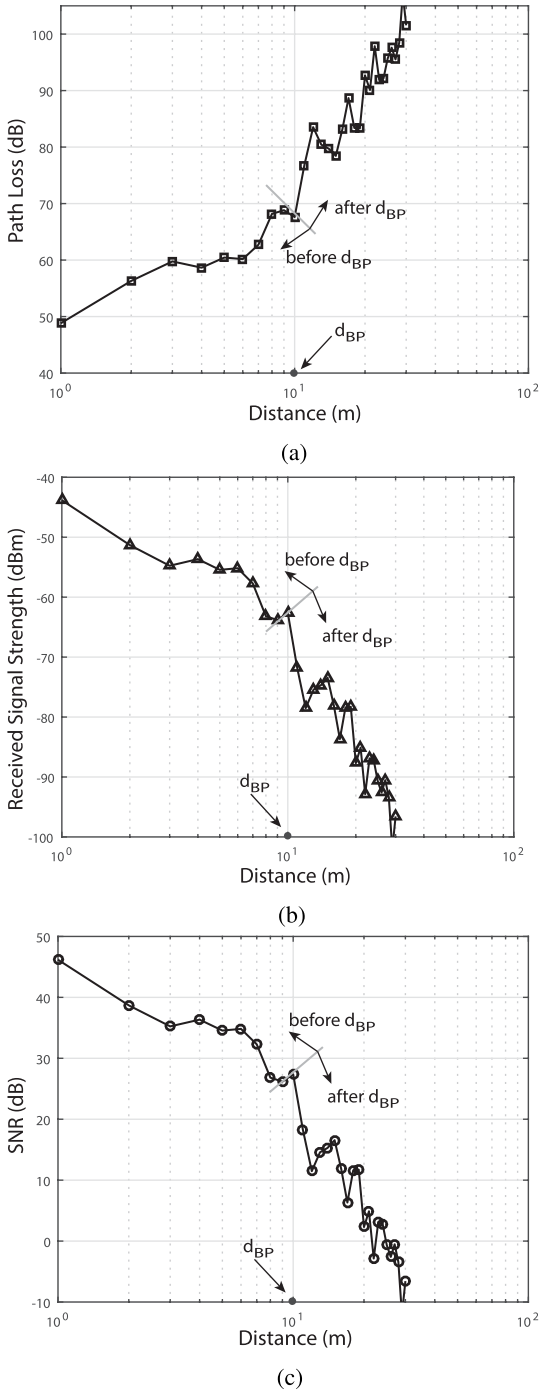

FIGURE 13. Loss in the received signal as a function of distance. (a) Path Loss. (b) RSS. (c) SNR.

Thus based on a specific channel model as illustrated in TABLE 8, the path loss, RSS, and SNR can be calculated. For example for TGn channel D, the path loss, RSS values, and SNR are calculated in Fig. 13a, Fig. 13b, and Fig. 13c respectively. We assume unit antenna gains at transmitter and receiver, thus $G_t = G_r = 1$. Similarly, the values of λ is determined from the carrier frequency of 802.11ac which is $f_c = 5.23GHz$, therefore C/λ where C is the speed of

TABLE 8. Path loss parameters for TGn channel models 802.11.

Channel Model	d_{BP} (m)	Slope before d_{BP}	Slope after d_{BP}	Shadow Fading Std. dev(dB) before d_{BP} (LOS)	Shadow Fading Std. dev(dB) after d_{BP} (NLOS)
A	5	2	3.5	3	4
B	5	2	3.5	3	4
C	5	2	3.5	3	5
D	10	2	3.5	3	5
E	20	2	3.5	3	6
F	30	2	3.5	3	6

electromagnetic waves i.e., $C = 3 \times 10^8$m/s. The values of d_{BP} and σ for channel D are taken from TABLE 8. Note that the slope and σ are different before and after d_{BP}. The $PL(d)$ in dBm for a T-R separation of d (in m) is calculated from eq. (22). We assume that the transmitter power is $+5$dBm and the noise at the receiver is equal to the noise floor value of -90dBm. Consequently using the values of $PL(d)$ and $P_t = 5$dBm in eq. (21), the RSS value E is determined. Lastly, substituting E and $W = -90$dBm in eq. (19), the SNR value X is calculated at the receiver (client).

REFERENCES

[1] A. Asadi, Q. Wang, and V. Mancuso, "A survey on device-to-device communication in cellular networks," *IEEE Commun. Surveys Tuts.*, vol. 16, no. 4, pp. 1801–1819, 4th Quart., 2014.

[2] *P2P Technical Group, Wi-Fi Peer-to-Peer (P2P) Technical Specification v1.0*, Wi-Fi Alliance, Santa Clara, CA, USA, Dec. 2009.

[3] G. Fodor, S. Parkvall, S. Sorrentino, P. Wallentin, Q. Lu, and N. Brahmi, "Device-to-device communications for national security and public safety," *IEEE Access*, vol. 2, pp. 1510–1520, Dec. 2014.

[4] R. Rajadurai, K. S. Gopalan, M. Patil, and S. Chitturi, "Enhanced interworking of LTE and WI-FI direct for public safety," *IEEE Commun. Mag.*, vol. 54, no. 4, pp. 40–46, Apr. 2016.

[5] G. Z. Khan, R. Gonzalez, E.-C. Park, and X.-W. Wu, "A reliable multicast MAC protocol for Wi-Fi direct 802.11 networks," in *Proc. Eur. Conf. Netw. Commun. (EuCNC)*, Jun. 2015, pp. 224–228.

[6] A. Kamilaris and A. Pitsillides, "Mobile phone computing and the Internet of Things: A survey," *IEEE Internet Things J.*, vol. 3, no. 6, pp. 885–898, Dec. 2016.

[7] K. Abboud, H. A. Omar, and W. Zhuang, "Interworking of DSRC and cellular network technologies for V2X communications: A survey," *IEEE Trans. Veh. Technol.*, vol. 65, no. 12, pp. 9457–9470, Dec. 2016.

[8] *IEEE 802.11ac-Enhancements for Very High Throughput for Operation in Bands Below 6 GHz*, Standards IEEE P802.11ac/D5.0, 2013.

[9] J. Vella and S. Zammit, "A survey of multicasting over wireless access networks," *IEEE Commun. Surveys Tuts.*, vol. 15, no. 2, pp. 718–753, 2nd Quart., 2013.

[10] S. Jang and S. Bahk, "A channel allocation algorithm for reducing the channel sensing/reserving asymmetry in 802.11ac networks," *IEEE Trans. Mobile Comput.*, vol. 14, no. 3, pp. 458–472, Mar. 2015.

[11] J. Oueis, V. Conan, D. Lavaux, R. Stanica, and F. Valois, "Overview of LTE isolated E-UTRAN operation for public safety," *IEEE Commun. Mag.*, vol. 1, no. 2, pp. 98–105, Feb. 2017.

[12] Z. Kaleem, Y. Li, and K. Chang, "Public safety users' priority-based energy and time-efficient device discovery scheme with contention resolution for ProSe in third generation partnership project long-term evolution-advanced systems," *IET Commun.*, vol. 10, no. 15, pp. 1873–1883, Oct. 2016.

[13] Z. Kaleem and K. Chang, "Public safety priority-based user association for load balancing and interference reduction in PS-LTE systems," *IEEE Access*, vol. 4, pp. 9775–9785, 2016.

[14] Y. Duan *et al.*, "Wi-Fi direct multi-group data dissemination for public safety," in *Proc. World Telecommun. Congr.*, Berlin, Germany, 2014, pp. 1–6.

[15] J. Kuri and S. K. Kasera, "Reliable multicast in multi-access wireless LANs," in *Proc. 18th Annu. Joint Conf. IEEE Comput. Commun. Soc.*, New York, NY, USA, Mar. 1999, pp. 760–767.

[16] Y. Seok and T. Turletti. (2006). "Practical rate-adaptive multicast schemes for multimedia over IEEE 802.11 WLANs," INRIA, Paris, France, Tech. Rep. 5993. [Online]. Available: http://hal.inria.fr/inria-00104699/en/

[17] Y. Park, Y. Seok, N. Choi, Y. Choi, and J.-M. Bonnin, "Rate-adaptive multimedia multicasting over IEEE 802.11 wireless LANs," in *Proc. 3rd IEEE Consum. Commun. Netw. Conf. (CCNC)*, vol. 1. Jan. 2006, pp. 178–182.

[18] N. Choi, Y. Seok, T. Kwon, and Y. Choi, "Multicasting multimedia streams in IEEE 802.11 networks: A focus on reliability and rate adaptation," *Wireless Netw.*, vol. 17, no. 1, pp. 119–131, 2011.

[19] J. Villalon, P. Cuenca, L. Orozco-Barbosa, Y. Seok, and T. Turletti, "ARSM: A cross-layer auto rate selection multicast mechanism for multi-rate wireless LANs," *IET Commun.*, vol. 1, no. 5, pp. 893–902, Oct. 2007.

[20] D. Camps-Mur, A. Garcia-Saavedra, and P. Serrano, "Device-to-device communications with Wi-Fi Direct: Overview and experimentation," *IEEE Wireless Commun.*, vol. 20, no. 3, pp. 96–104, Jun. 2013.

[21] *Wi-Fi Peer-to-Peer*. Accessed: Mar. 7, 2017. [Online]. Available: https://www.android.com/developers

[22] *AirDrop*. Accessed: Mar. 7, 2017. [Online]. Available: http://www.apple.com/developer

[23] *IEEE Standard for Wireless LAN Medium Access Control (MAC) and Physical Layer (PHY) Specifications*, Standard 802.11-2007, Jun. 2007.

[24] S. W. Kim, B. S. Kim, and Y. Fang, "Network allocation vector (NAV)-based opportunistic prescanning process for WLANs," *Electron. Lett.*, vol. 46, no. 24, pp. 1630–1632, Nov. 2010.

[25] M. Evans, N. Hastings, and B. Peacock. *Statistical Distributions*. Hoboken, NJ, USA: Wiley, 2000, pp. 102–105.

[26] *TGn Channel Models*, Standard IEEE 802.11-03/940r4, May 2004. [Online]. Available: http://mentor.ieee.org/802.11/dcn/03/11-03-0940-04-000n-tgn-channel-models.doc

[27] S. Cho *et al.*, *MIMO-OFDM Wireless Communications With MATLAB*. Hoboken, NJ, USA: Wiley, 2010.

[28] D. Halperin, W. Hu, A. Sheth, and D. Wetherall, "Predictable 802.11 packet delivery from wireless channel measurements," in *Proc. ACM SIGCOMM*, 2010, pp. 159–170.

[29] P. Kyritsi, R. A. Valenzuela, and D. C. Cox, "Channel and capacity estimation errors," *IEEE Commun. Lett.*, vol. 6, no. 12, pp. 517–519, Dec. 2002.

GUL ZAMEEN KHAN (M'16) received the Bachelor's degree in computer systems engineering from the University of Engineering and Technology, Peshawar, Pakistan, in 2007, and the Master's degree in computer engineering from Hanyang University, South Korea, in 2011. He is currently pursuing his Ph.D. studies in the School of ICT, Griffith University Australia.

He was a Lab Engineer with the Ghulam Ishaq Khan Institute of Engineering Sciences and Technology, Pakistan. He was also a faculty member at the Sarhad University of IT, Peshawar, Pakistan, and the COMSATS Institute, Abbottabad, Pakistan. He was a Research Assistant with the Wireless Networks Laboratory, Dongguk University, South Korea. His areas of interest are MAC and PHY layers analysis of 802.11, multicast in Wi-Fi direct networks, wireless sensor networks, and wireless body area networks.

Mr. Khan is a Professional Member of the Pakistan Engineering Council and an active member of the Institute of Integrated and Intelligent Systems, Griffith University, Australia.

EUN-CHAN PARK (M'01) received the B.S., M.S., and Ph.D. degrees from the School of Electrical Engineering and Computer Science, Seoul National University, Seoul, South Korea, in 1999, 2001, and 2006, respectively.

He was with Samsung Electronics, South Korea, as a Senior Engineer, from 2006 to 2008. He is currently an Associate Professor with the Department of Information and Communication Engineering, Dongguk University, Seoul, where he is also the Head of the Wireless Networks Laboratory. His research interests include performance analysis, resource allocation, quality of service, congestion control, and cross-layer optimization in wired and wireless networks.

Dr. Park is a member of the IEEE Communications Society.

RUBEN GONZALEZ (M'94) received the B.E. and Ph.D. degrees from the University of Technology, Sydney (UTS). He is currently a Senior Lecturer with the School of ICT, Griffith University, Australia, where he is also the Director of the Bachelor of Computer Science.

He was the Founder and the CTO of ActiveSky Inc., a wireless media technology company, and has also held research positions at Wollongong University, OTC Ltd Research Labs, and UTS. He has also held software engineering positions at various private enterprises.

He has over 80 refereed publications and a number of patents. He is a member of the Institute for Integrated and Intelligent Systems and Griffith University.